RSC Advances

PAPER

View Article Online
View Journal | View Issue

Cite this: *RSC Adv.*, 2026, **16**, 18342

Eco-friendly carbon dot-based nanocomposites in smart construction materials for green-house gases reduction

Basel Abd Elshafy,[a] Mahmoud Hazem,[b] Heba El-Shafey,[a] Omar Mbrouk *[ac] and Hoda Hafez[ad]

Advanced composites and hybrid nanomaterials for environmental applications such as CO_2 capture could be a promising approach to addressing the impacts of climate change. One of the most promising zero-dimensional nanomaterials is carbon dots (CDs), which are carbonaceous nanomaterials whose particle sizes range from 1 to 10 nm. This study investigates environmentally friendly and novel carbon dot nanocomposites (CD-NCs), including TiO_2, ZnO, and SiO_2 semiconductor nanoparticles (SNs), in Portland cement (OPC) to be converted to new smart construction materials for reducing CO_2 emissions. Water-soluble CDs were made *via* microwave hydrothermal synthesis, forming 6–10 nm spheres. Optical properties revealed photoluminescence emission at 490 nm. Different molar ratios of CDs are introduced into the SNs to produce *x*% CD-TiO_2, CD-ZnO, and CD-SiO_2 (x = 0.01, 0.05, and 1% molar ratio). XRD, XPS, and TEM techniques evidenced the integration of CDs without modification in the crystallite size of host materials. CDs and their cement composites improved compressive strength and bulk density while lowering porosity, leading to enhanced hydration and better mechanical performance. Adding CDs to the nanoparticle matrix improved S_{BET} and XPS surface features, increasing oxygen vacancies. The nanocomposite cement's CO_2-removal performance and reuse were tested under simulated sunlight. The cement-based CDs nanocomposites show activity and reusability for three repetitive cycles, demonstrating their significance for CO_2 capturing.

Received 6th February 2026
Accepted 14th March 2026

DOI: 10.1039/d6ra01080f

rsc.li/rsc-advances

1 Introduction

In line with the COP27 and Egypt's 2030 strategy to achieve a clean environment through green technology to overcome the climate change phenomenon, the research-driven technology of this work aims to introduce smart self-cleaning building materials into the construction industry.[1,2] Nanotechnology is the manipulation of materials with a size between 1 and 100 nm. The goal of the multidisciplinary field of nanotechnology is to create new and enhanced materials with important physical and chemical properties and functionalities.[2] The characteristics of material at this size are different from those of the same substance at greater dimensions.[3] This enables investigation of a wide range of novel nanotechnology applications across several fields. Nanotechnology is a promising area across agriculture, water remediation, medicine, electronics, and many industrial sectors, including energy and construction. With the fast growth of technology, the industrial applications of nanotechnology have observed tremendous growth in the last few years.[3]

The construction industry is a major global sector, crucial to national economies and development. It consumes approximately 40% of global energy and 50% of total resources, making it a key indicator of a country's economic health. By transforming resources into economic and social infrastructure, the construction industry significantly boosts economic performance and national welfare, contributing around 5–9% to the gross domestic product (GDP) in developing countries.[4,5]

In recent years, the building industry has attempted to augment traditional construction materials using nanotechnology.[1,3,4,6,7] Nanotechnology is a novel approach in smart construction materials. Many nanomaterials, including zero-dimensional (*e.g.*, nanoparticles), one-dimensional (*e.g.*, nanorods or nanotubes), or two-dimensional (usually realized as thin films or stacks of thin films), have been incorporated as additives in construction materials.[8,9] The integration of different types of nano-additives into conventional cement, the most frequently consumed manufactured material in civil engineering, to create nanoparticles enhanced cement-based

[a]*Nanotechnology and Its Environmental Applications Department, Environmental Studies and Research Institute (ESRI), University of Sadat City (USC), Sadat City, Egypt. E-mail: basel.abdelshafy@esri.usc.edu.eg; heba.shafey@esri.usc.edu.eg; omar.mbrouk@esri.usc.edu.eg; hoda.hafez@esri.usc.edu.eg*

[b]*Faculty of Science, Ain Shams University, Cairo, Egypt. E-mail: m.m.hazem@sci.asu.edu.eg*

[c]*Alexandria Drinking Water Company (AWCO), 61 El-Horreya Avenue, Alexandria, Egypt*

[d]*Faculty of Science, University of Sadat City (USC), Sadat City, Egypt*

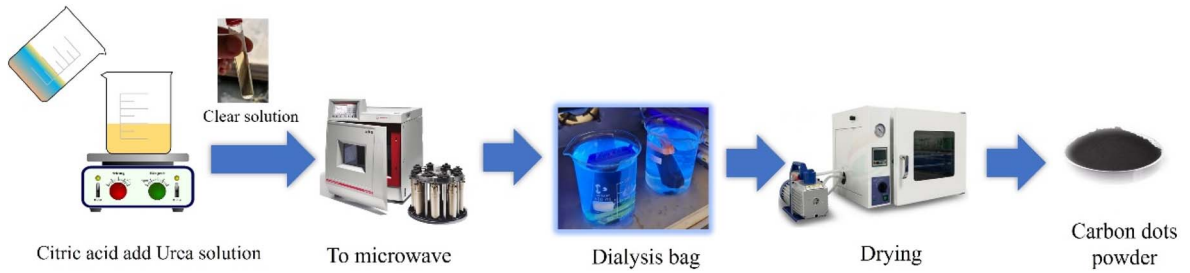

Fig. 1 A schematic representation of the preparation method of carbon dots powder.

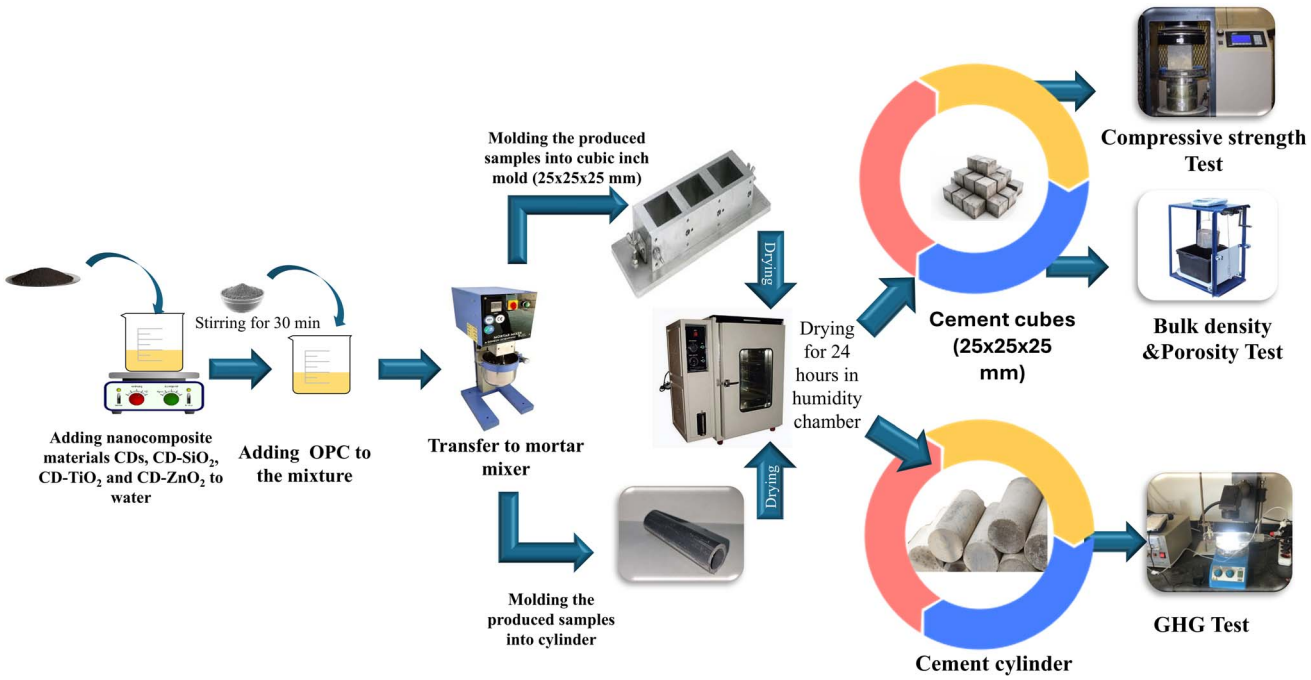

Fig. 2 Schematic representation of the preparation method for modified cement materials mixed with different nanocomposites.

composites with enhanced characteristics, has been one of the great advances of nanotechnology in materials research.[10–12] Except for traditional nanomaterials such as nano-silica[13,14] and nano aluminum[15,16] *etc.*, carbon based nanomaterials (CBN) including carbon black,[17–20] carbon nanofibers (CNFs)[21] carbon nanotubes (CNTs),[22–24] graphene,[25–27] graphene nanoplates (GNPs),[25,28] graphene oxide (GO)[29] and reduced graphene oxide (rGO)[29–31] have been attracting increasing amounts of research attention in terms of enhancing the mechanical, electrical and physical properties of construction materials. Carbon-based nanomaterials (CBNs) are mainly composed of carbon atoms with a high aspect ratio or specific surface area, low density, and unique physical and chemical properties[32–34] CBNs, including GO and rGO, can provide new functions, including thermal electrical interfacing,[29,35,36] self-cleaning,[37,38] electromagnetic shielding,[39] and self-sensing.[40] For example, CBNs can be added to cement-based materials at very low ratios (usually below 0.50 wt%) to serve as additional seeding sites, producing durable, sustainable composites with enhanced mechanical

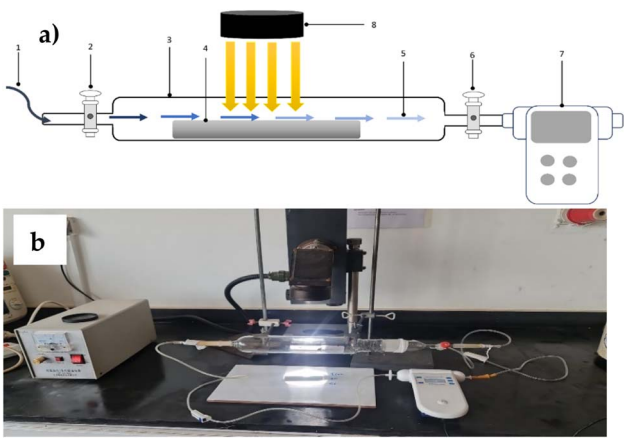

Fig. 3 (a) Schematic diagram: 1 – gas source, 2 – gas inlet tap, 3 – reactor tube chamber, 4 – modified cement with nanocomposite, 5 – purified gas, 6 – gas outlet tap, 7 – gas detector, 8 – light source. (b) Photo image of the photoreactor for GHG removal.

properties.[41–43] CBNs can enhance cement-based composites and enable new functions, such as stress sensing and temperature monitoring, depending on the type of nanomaterial added.[44–46] Moreover, the application of CBNs in cement manufacturing can also help reduce greenhouse gas (GHG) emissions in the atmosphere and provide a sustainable, eco-friendly approach.[47] Carbon dots (CDs) have attracted attention for their outstanding corrosion resistance, chemical stability, low cost, durability, and non-toxicity, and also exhibit adjustable luminescent properties.[48] Presently, CDs are widely used across various fields, including electrochemistry, catalysis, and photovoltaics. Nevertheless, there are few reports on its application in construction materials.[49,50] Carbon Dots (CDs) are distinguished by their extremely small size in the nanometre range and their large specific surface area, which enables them to disperse well in the cement matrix and fill micro-voids, thus increasing density and reducing porosity in the concrete structure.[51] Moreover, these CDs nanoparticles can play a role in nucleation during the hydration reaction between cement and water, thereby favouring the formation of hydration products more regularly and densely, which, in turn, increases the strength and stiffness of the concrete material.[49,52] The presence of hydrophilic functional groups, such as carboxyl and amine groups, on the new surface of CDs, which is a phenomenon, increases the bonding capacity between the CDs and cement particles and helps the development of hydration crystals, leading to an increase in the strength of the concrete material. Furthermore, CDs exhibit excellent dispersion in aqueous solution, relatively low production costs compared with other nanoparticles, such as graphene or carbon nanotubes, and low toxicity, making them a promising material for improving the properties of Portland cement in smart and sustainable construction.[53,54] Herein, in this work of research, environmentally friendly CD nanocomposites (CD-NCs) from CDs-TiO_2, CDs-ZnO, and CDs-SiO_2 have been synthesized *via* a green chemistry approach using a simple and fast microwave-assisted hydrothermal method under optimized conditions. This is in order to achieve an integrated ecosystem based on clean technology for a clean environment. These promising materials have been applied in cement building materials and applied for

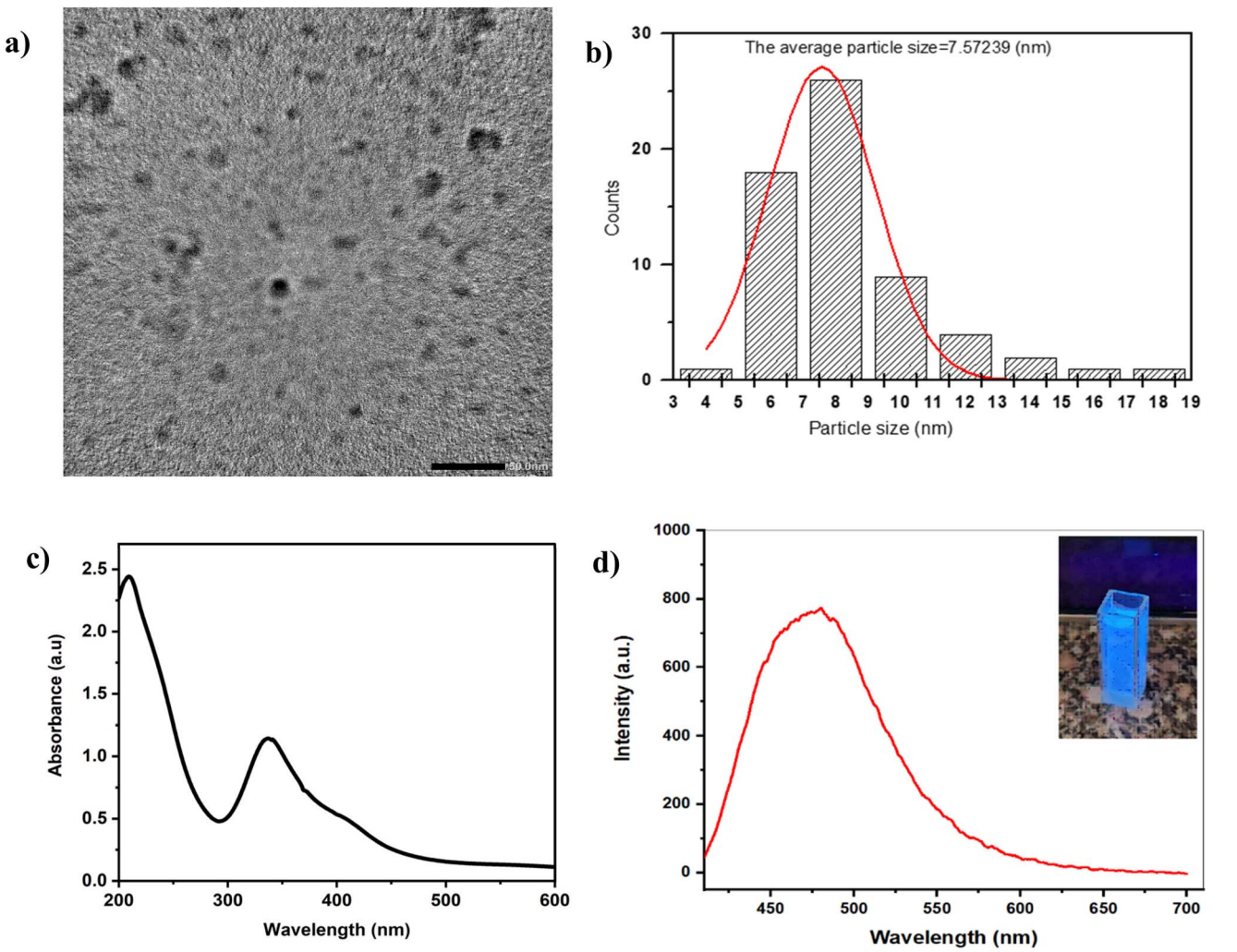

Fig. 4 (a) The TEM image of the CDs. (b) The histogram of the size distribution for CDs. (c) Absorbance and (d) photoluminescence spectra for CDs.

the first time in CO_2 reduction. The physicochemical, structural, optical, and toxicity of the new materials have been studied. From the point of view of sustainability, the reusability of modified building materials has been investigated for three repetitive cycles.

2 Experimental

2.1 Materials

Zinc acetate dihydrate (Zn $(CH_3COO)_2 \cdot H_2O$, LoBaChemie, >98%), titanium(IV), isopropoxide ($C_{12}H_{28}O_4Ti$, Sigma Aldrich, 97%), and tetraethyl orthosilicate (reagent grade, Sigma Aldrich, 98%) were used as precursors for synthesis of ZnO, TiO_2 and SiO_2 nanostructured materials using orange peel extract by our previous methods.[55,56] Urea granular $(CO(NH_2)_2$, Zchemicals 99%) and citric acid ($C_6H_8O_7$, LoBaChemie, 99.5%) have been used for the synthesis of carbon dots CDs. Ordinary Portland cement with a grade of 42.5 and ISO standard sand (ISO 679: 2009) was used to produce cement-based building materials.

2.2 Methods

2.2.1 Preparation of CDs. Water-soluble CDs have been synthesized *via* a modified microwave hydrothermal method.[51] In a typical method, a total of 1.50 g of citric acid and 0.50 g of urea were simultaneously added to 10.0 mL of deionized water with continuous stirring for 20 min, resulting in a clear, transparent solution. This solution was then subjected to microwave treatment using an Anton Paar Multiwave 5000 at 200 °C for 120 seconds. Afterward, a dark brown aqueous solution of carbon quantum dots was obtained and placed in a 3.5 kDa dialysis membrane bag for 24 hours. A transparent, yellow-colored CQD liquid was obtained. Finally, the CDs solution was dried at 90 °C under vacuum for 3 hours to get the powder. A schematic representation of the preparation method is given in Fig. 1.

2.2.2 Synthesis of CDs-ZnO, CDs-TiO_2 and CDs-SiO_2 nanocomposites. A green-synthesis approach of colloidal solutions from ZnO and TiO_2 nanomaterials is prepared using orange peel extract, according to our previous work.[55,56] For the SiO_2 colloidal solution, 250 mL of orange peel aqueous extract was combined with 20 mL of tetraethyl orthosilicate as the precursor and stirred at room temperature for 15 minutes. Then, 10 mL of ethanol was added, with stirring continued for an additional 15 minutes, followed by the addition of 12.5 mL of HCl under stirring. This process resulted in the formation of a gel-like precipitate. The different composites from CDs-TiO_2, CDs-ZnO, and CDs-SiO_2 nanomaterials have been synthesized using different weight ratios of the CDs nanoparticles, including (0.01, 0.05, and 1 wt% relative to the parent nanomaterial), which were added to the colloidal solutions of TiO_2, ZnO, and SiO_2. The mixture of nanocomposites will be transferred into the microwave vessels and autoclaved at 90 °C for 30 minutes, dried at 90 °C for 1 hour, and finally heat-treated at 450 °C for 1 hour.[57]

2.2.3 Fabrication of modified cement cubes and tubes. A control cement paste was prepared by mixing ordinary Portland cement (OPC) with water at a water-to-cement ratio (W/C) of 0.29, using a mortar mixer in accordance with EN 196-1.[58] Modified cement samples were then prepared by incorporating

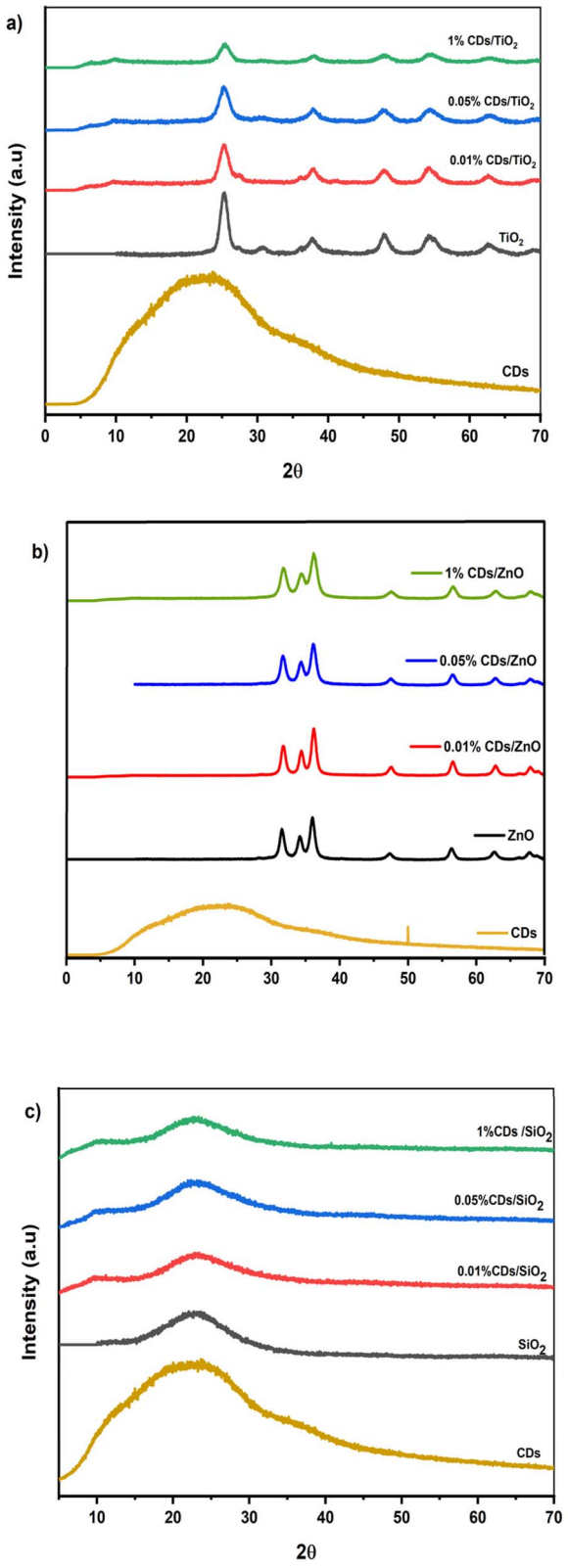

Fig. 5 XRD patterns of (a) CDs/TiO_2, (b) CDs/ZnO, and (c) CDs/SiO_2 nanocomposites.

Table 1 Physico-chemical characteristics of the different CD-NCs, including crystallite sizes, specific surface area (S_{BET}), average pore diameter (nm), and total pore volume ($cm^3\ g^{-1}$)

Sample	Average crystallite size (nm)	S_{BET} ($m^2\ g^{-1}$)	Average pore diameter (nm)	Total pore volume ($cm^3\ g^{-1}$)
TiO_2	7.2	125.74	5.756	0.1810
0.01% CDs/TiO_2	7.5	166.9	6.7334	0.2809
0.05% CDs/TiO_2	6.2	156.93	3.855	0.1512
1% CDs/TiO_2	6.5	150.75	6.6987	0.2525
ZnO	13.0	33.80	27.164	0.2296
0.01% CDs/ZnO	13.2	31.01	32.857	0.2547
0.05% CDs/ZnO	14.0	42.71	31.583	0.3373
1% CDs/ZnO	10.5	44.70	29.700	0.3319
SiO_2	13.2	403.61	2.2807	0.2301
0.01% CDs/SiO_2	15.5	496.75	2.9688	0.3687
0.05% CDs/SiO_2	13.5	503.76	2.9720	0.3743
1% CDs/SiO_2	14.9	459.14	3.5264	0.3933

synthesized CD-nanocomposite materials (CD-NCs), including CD-TiO_2, CD-ZnO_2, and CD-SiO_2, by varying concentrations (0.01, 0.05, 0.1, and 1 wt%), following the method of J. Zhang and H. Qu, S. Qian, and their coworkers.[50,51] A schematic of the procedure is provided in Fig. 2. The process begins with the addition of synthesized nanomaterials (CDs, CD-TiO_2, CD-ZnO_2, and CD-SiO_2) to water, followed by stirring for 30 minutes.

Ordinary Portland cement (OPC) is then added to the mixture, which is subsequently transferred to a mortar mixer. The mixed paste is molded into cubic ($25 \times 25 \times 25$ mm) and cylindrical molds of height ($h = 100$ mm) and diameter ($d =$ 12.5 mm). The molded samples were kept overnight in a humidity chamber (RH $\sim$ 99%) to prevent dryness of the prepared paste. After 24 hours, the hardened cubic samples were then demoulded and cured under water for 3, 7, and 28 days from the mixing day, while the cylindrical molds were kept under water for 28 days, then demolded for measurements and application.

2.3 Characterization

The structural and chemical identification of the nanocomposites has been obtained by X-ray photoelectron

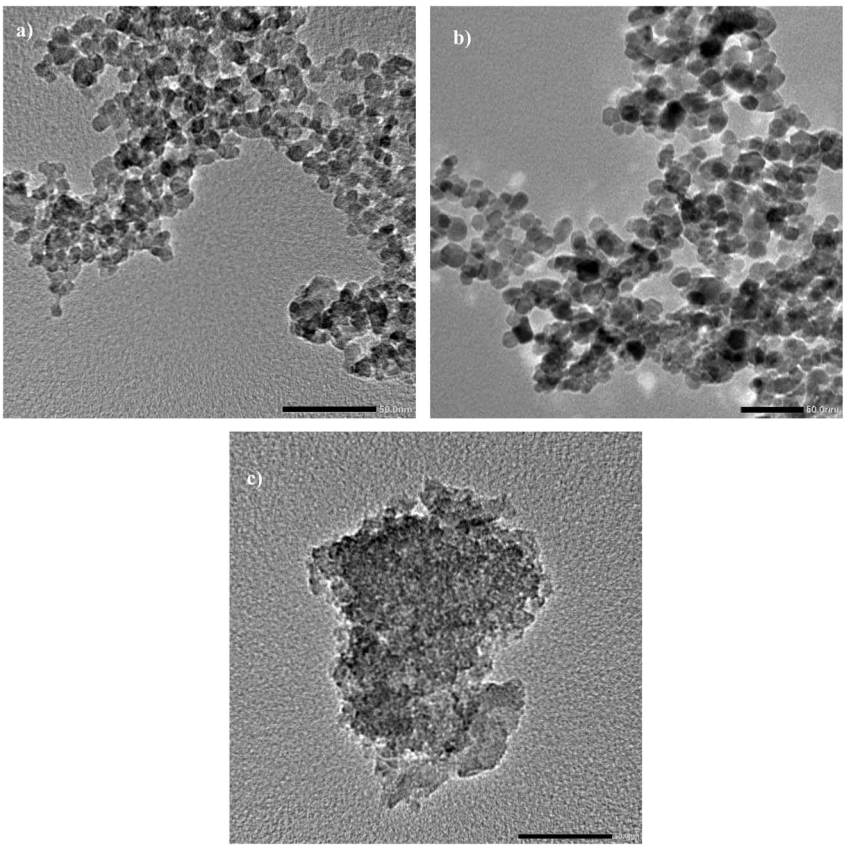

Fig. 6 TEM images of (a) CDs/TiO_2; (b) CDs/ZnO, and (c) CDs/SiO_2 nanocomposites.

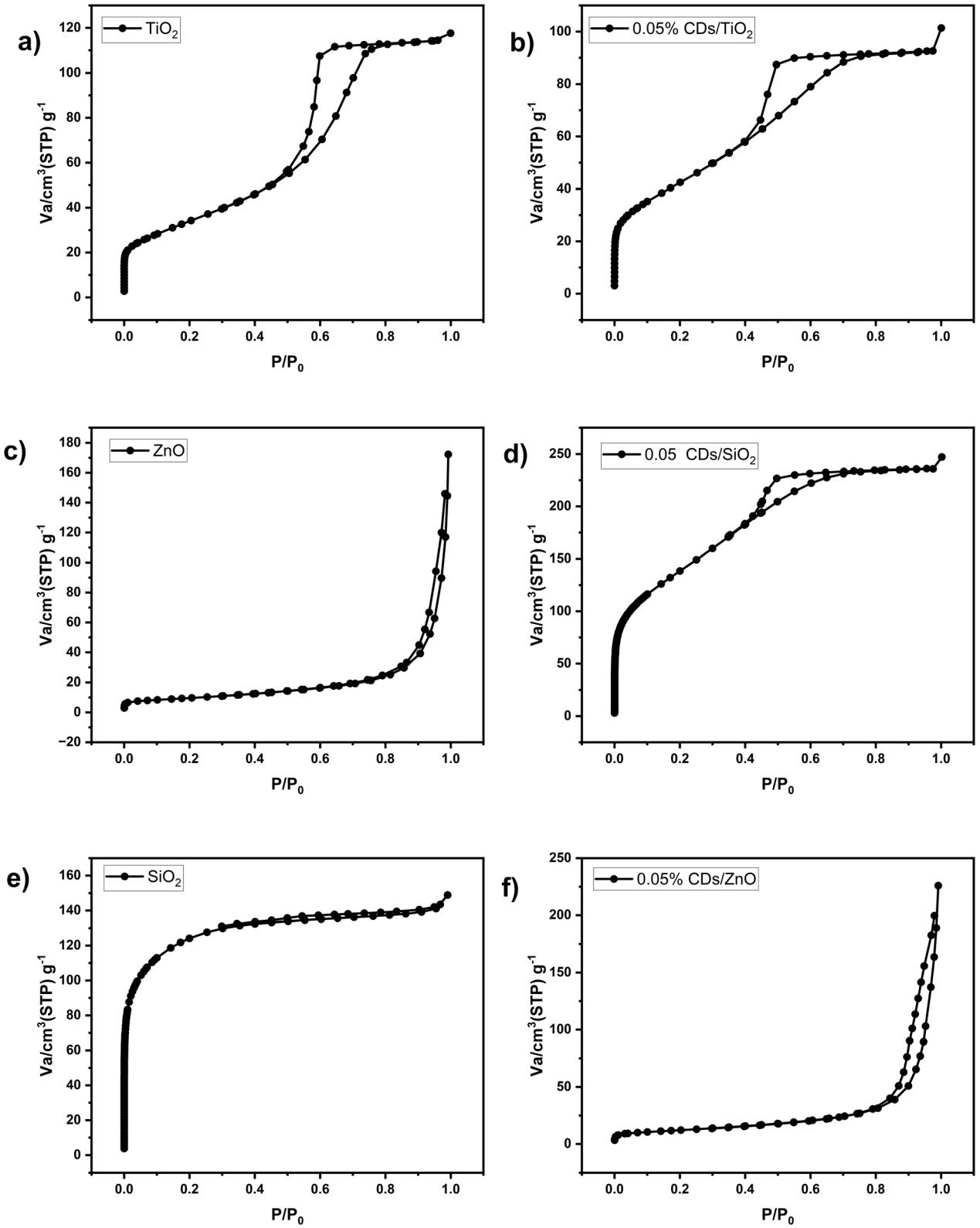

Fig. 7 Adsorption–desorption isotherms (N_2 at 77 K) of (a) TiO_2, (b) 0.05% CDs/TiO_2, (c) ZnO, (d) 0.05 CDs/SiO_2, (e) SiO_2, and (f) 0.05% CDs/ZnO, showing surface area and pore structure characteristics.

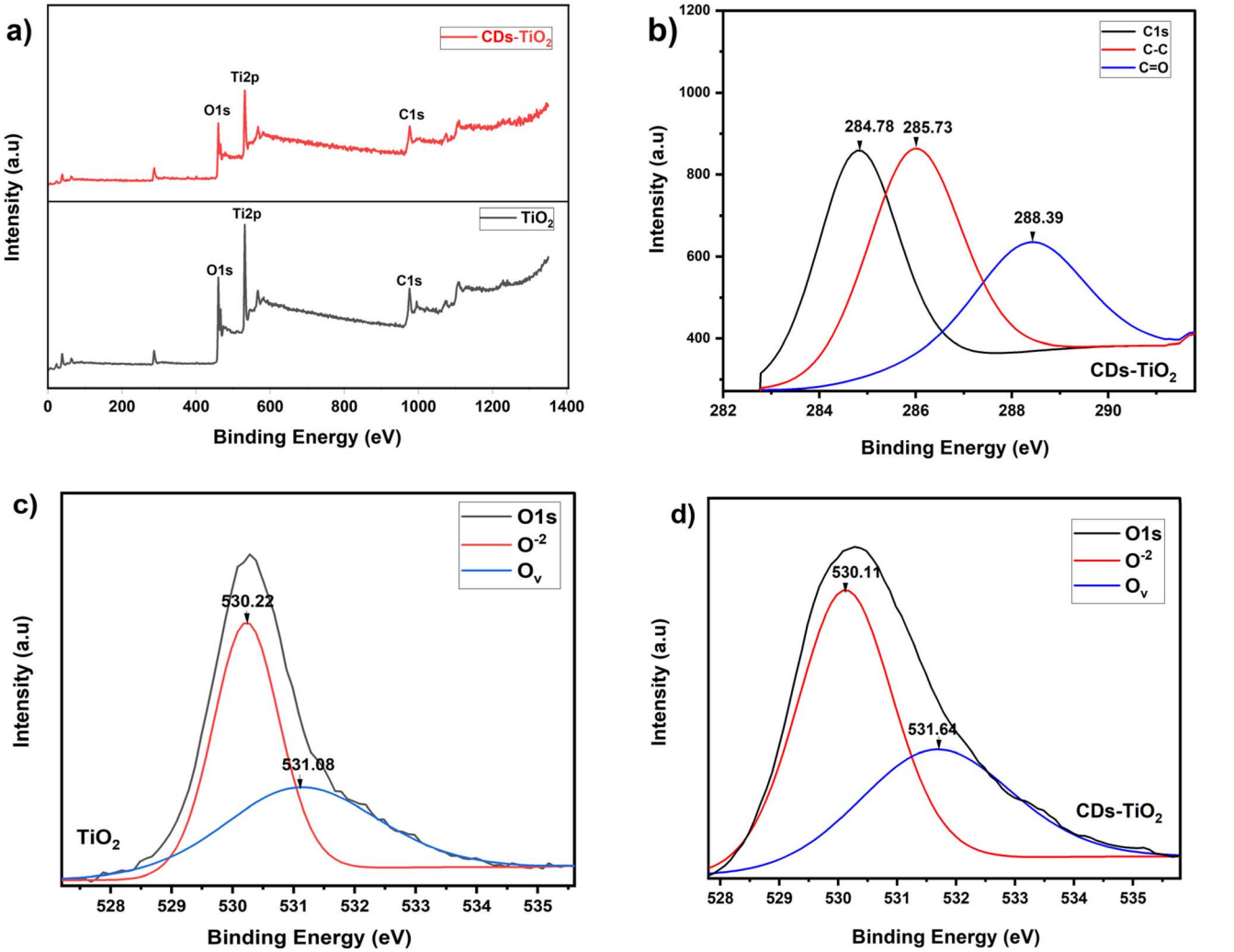

Fig. 8 XPS spectra of CDs-TiO_2 nanocomposite: (a) survey spectra, (b) C 1s, and (c and d) O 1s spectra.

spectroscopy (XPS, AXIS ULTRA, Kratos Analytical Ltd) and X-ray powder diffraction analysis (XRD, Bruker D8 Advance X-ray diffractometer, Cu Kα radiation [$\lambda = 1.5406$ Å] at 10 kV and 10 mA). The microscopic investigation has been done by a high-resolution transmission electron microscope (HR-TEM, JEOL, JEM-2100, Tokyo, Japan). Surface properties have been examined by an automatic surface area and pore size analyzer (BELSORP MINI X) to determine specific surface area (S_{BET}) and pore size distribution (Barrett–Joyner–Halenda [BJH] method) *via* adsorption–desorption of N_2 gas at 77 K. The optical properties of the nanoproducts were analyzed using a Shimadzu 2600 diffuse reflectance spectrometer and a PerkinElmer LS55 Luminescence Spectrometer (USA).

2.4 Photocatalytic reduction and capturing setup

The CO_2 photocatalytic reduction and capturing experiments using the modified OPC samples were carried out in a designed photoreactor at Nano-Phochem. Lab, at Nanotech Dept., Environmental Studies and Research Institute (ESRI), USC (Fig. 3). The experimental setup of the photoreactor consists of a transparent glass cylinder of total volume 1.88 L. A xenon arc UV-vis Solar Simulator (CHF-XM500, Trusttech. Co., Ltd, China) is used for illumination of the cylindrical tube.

The system's intensity was adjusted to one sun (100 mW cm^{-2}) using a TENMARS (TM-2060) solar power meter. Gas-phase carbon dioxide concentration inside the reactor was continuously monitored using an Aeroqual gas detector (Model 300, Aeroqual Ltd, New Zealand), which was connected directly to the outlet of the photocatalytic reactor.

The device operates based on an electrochemical sensor, providing high-sensitivity detection of CO_2 in real time, with a detection range of 0–5000 ppm and an accuracy of ±5%. Data was recorded at different time intervals during light exposure of the modified OPC samples in a CO_2 environment.

3 Results and discussion

3.1 Optical and morphological characteristics of CDs

The optical and morphological structures of the prepared carbon dots were analyzed by TEM. The TEM image (Fig. 4a)

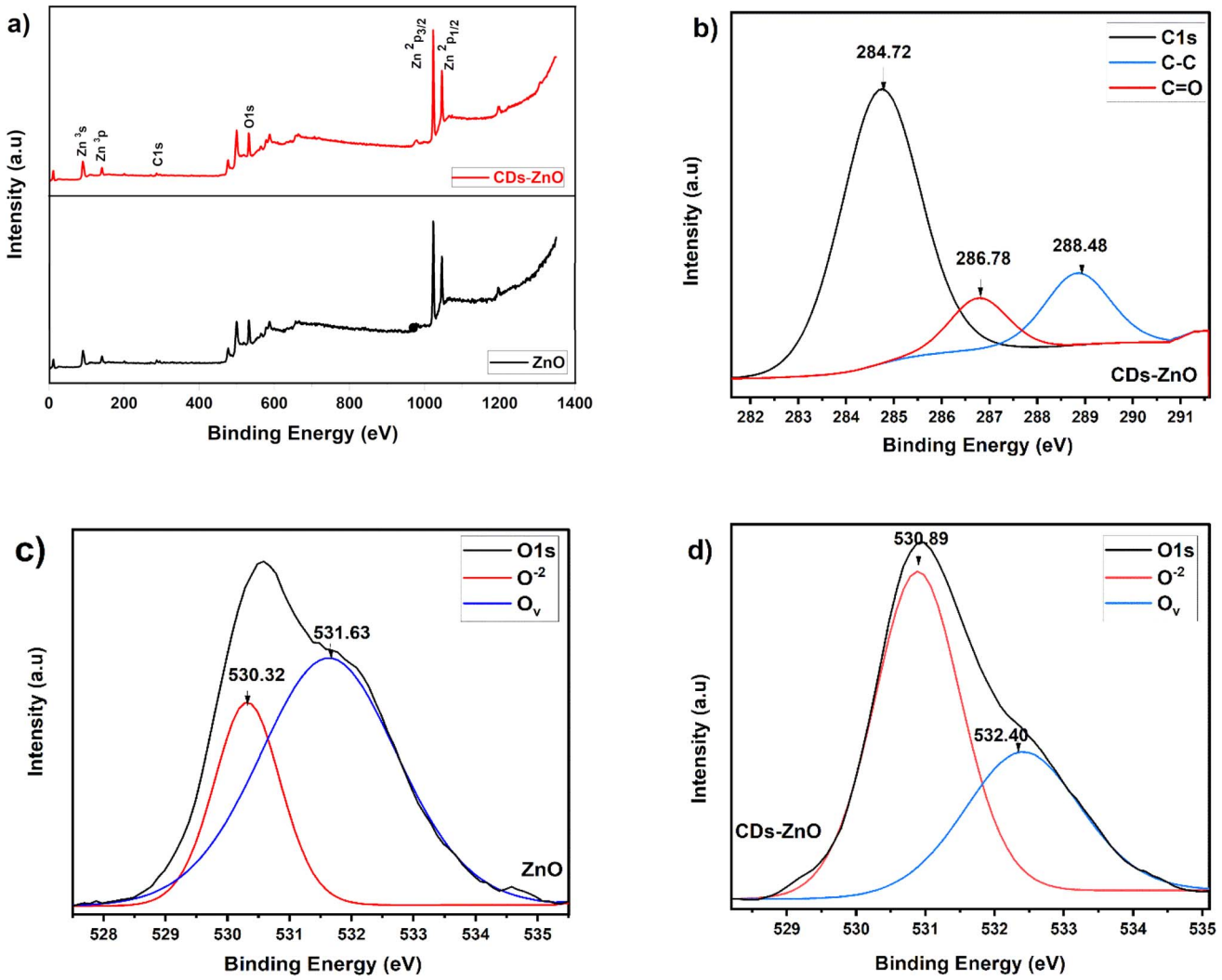

Fig. 9 XPS spectra of CDs-ZnO nanocomposite: (a) survey spectra, (b) C 1s, and (c and d) O 1s spectra.

shows the spherical structure of CDs nanoparticles that exhibit a uniform distribution in water, with no signs of aggregation, indicating their excellent dispersion.

The average particle size determined from the histogram of the CDs nanoparticles, Fig. 4b, was from 6–10 nm. The optical properties of the as-synthesized CDs are revealed by the UV-vis absorption and emission spectra and are shown in Fig. 4c and d. The absorption spectrum showed a broad band at $\lambda_{max} = 337$ nm, which can be attributed to the π–π* transition of the aromatic sp^2 (aromatic C=C bonds), with a long tail extending into the visible range.[59] The characteristic intense blue photoluminescence at 490 nm demonstrates the formation of CDs with a quantum yield = 14.9% using the relative fluorescence method with quinine sulfate as the reference sample (QY = 54% in 0.1 M H_2SO_4 at 380 nm), indicating that microwave-assisted synthesis was more efficient in terms of quantum yield.[60] The XRD spectrum of CDs in Fig. 5a displayed a broad peak located at the position 22.8° corresponding to the (002) plane of carbon, suggesting the existence of graphite carbon with an amorphous nature.[61]

3.2 Morphology, textural, and surface properties of the nanocomposites

Fig. 5 shows the X-ray diffraction patterns (XRD) of as-prepared CD-NCs. The peak related to CDs is not visible in all the nanocomposites due to low contents and weak crystallinity. The average crystallite sizes of the different nanocomposites using Sherre's Equation[62] are given in Table 1. It can be considered that the introduction of these small weight ratios from CDs has no significant effect on the crystallite sizes of the hosting materials (TiO_2, ZnO, and SiO_2). The TEM images of 0.05 wt% of CDs-TiO_2, CDs-ZnO, and CDs-SiO_2 nanocomposites are given in Fig. 6a–c, respectively. Due to the very small size of the CDs, it cannot be observed. However, the EDX analyses in S1 confirm the presence of CDs in all the hosting materials. The surface properties of the nanocomposite were investigated from nitrogen gas adsorption–desorption isotherms by Brunauer–Emmett–Teller (BET) analysis at 77 K. Fig. 7 presents the adsorption–desorption isotherms of the 0.05% CDs, 0.05%

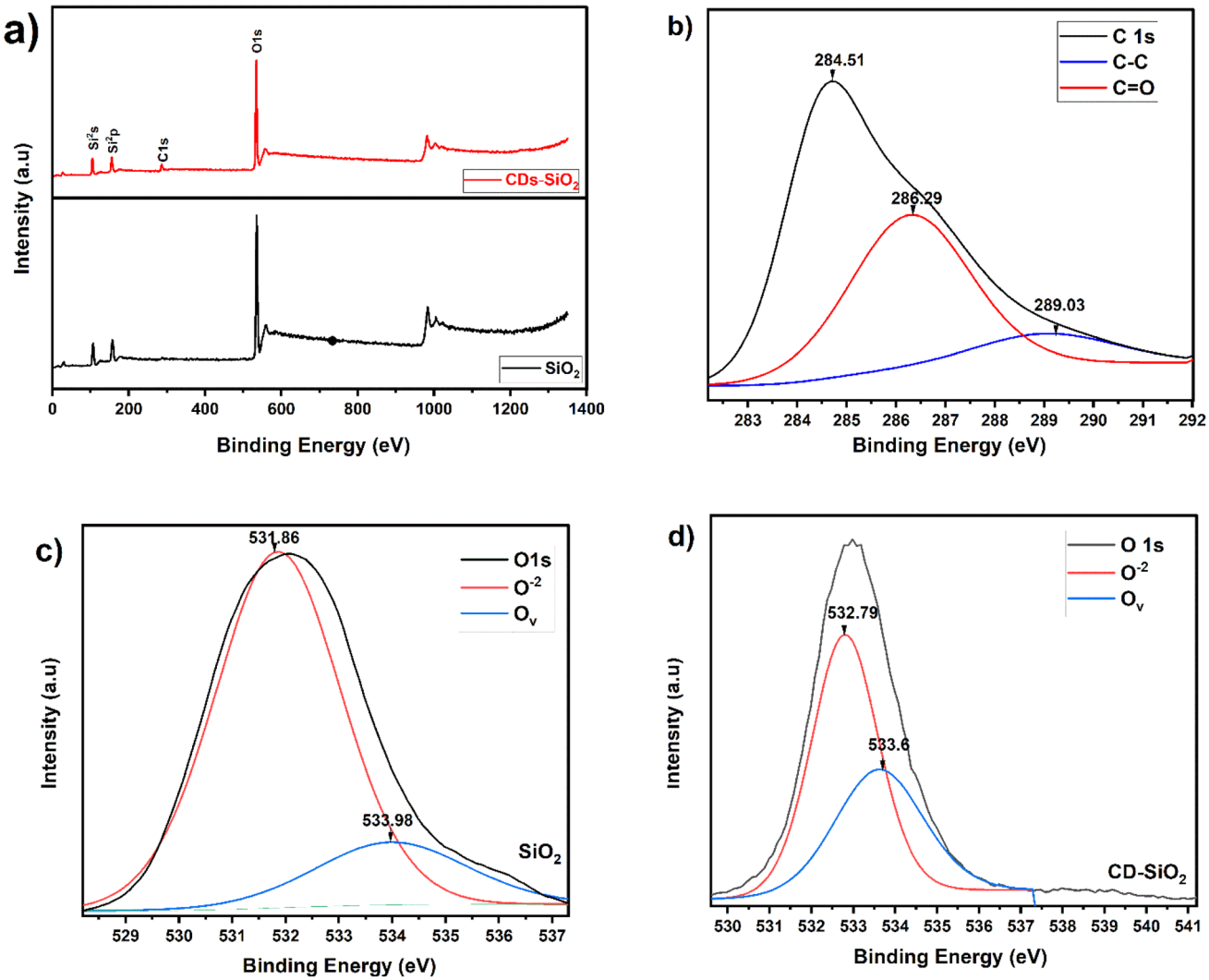

Fig. 10 XPS spectra of CDs-SiO_2 nanocomposite: (a) survey spectra, (b) C 1s, and (c and d) O 1s spectra.

Table 2 XPS data, binding energy values, and atomic weight ratios of CDs-TiO_2, CDs-ZnO, and CDs-SiO_2

	O_v		O^{2-}		C 1s		C–C		C=O	
Sample	B.E (eV)	At%	B.E (eV)	At%	B.E (eV)	At%	B.E (eV)	At%	B.E (eV)	At%
TiO_2	530.22	56.36	531.08	43.64						
0.05% CDs-TiO_2	530.11	61.27	531.64	38.73	284.78	17.28	285.73	57.28	288.39	25.44
ZnO	530.32	28.42	531.68	71.58						
0.05% CDs-ZnO	530.89	63.58	532.40	36.42	284.72	73.77	286.78	10.25	288.84	15.98
SiO_2	531.86	82.33	533.98	17.67						
0.05% CDs-SiO_2	532.79	61.42	533.60	38.58	284.51	45.43	286.29	44.41	289.03	10.16

CDs/ZnO, and 0.05% CDs/SiO_2 nanocomposites compared with their pure materials.

Based on Fig. 7, the TiO_2 and CDs/TiO_2 possess type IV adsorption isotherms with H2-hysteresis loops, which implies a mesoporous structure. However, ZnO and SiO_2 exhibit type II and type I isotherms, respectively. These isotherm types correspond to mesoporous and microporous structures (Table 1). From the results in Table 1, it can be well recognized that the specific surface area (S_{BET}) is generally increased by the incorporation of the CDs into the nanoparticle matrix. This may be due to the introduction of the small CDs into the metal oxide nanoparticles, thereby inhibiting the accumulation of metal oxide nanoparticles and enhancing the formation of oxygen vacancies in the host matrix[63]

XPS analyses presented in Fig. 8–10 have been used to provide convincing evidence for the surface states and

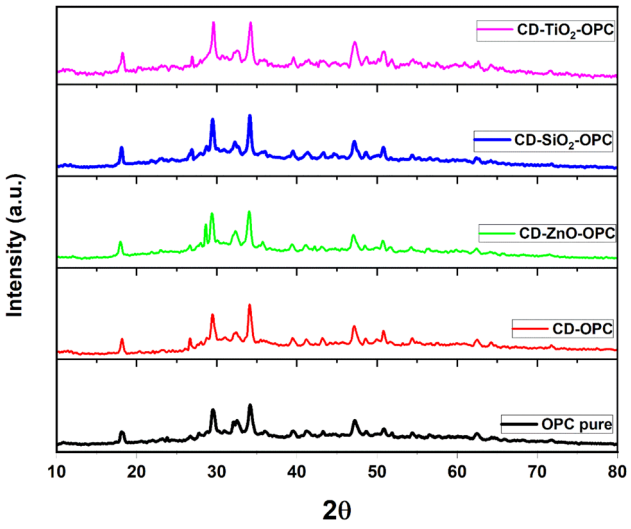

Fig. 11 XRD patterns of the modified cement materials with the different CD nanocomposites.

composition of the as-prepared CD-NCs. All the XPS data analyses are given in Table 2. The full survey spectrum of all the CD-NCs depicts the presence of carbon and oxygen elements, which further confirms the EDX analyses (S1).

The main characteristic peaks of C 1s in all the nanocomposites detected in the high resolution XPS spectra (Fig. 8b, 9b and 10b) are assigned to; non-oxygenated C (around 285 eV) and oxygenated carbon (around 288 eV) which are attributed to the C–C bonds with sp^2 orbital and C–O bonds with oxygen-rich groups, respectively.[64] For pure samples, the O 1s peaks (Fig. 8c, 9c, and 10c) are assigned to the lattice oxygen (O^{2-}) and surface oxygen vacancies (O_v).

In all nanocomposite samples, the O_v peak attributed to oxygen vacancies or defects shows an increase in its atomic% by incorporation of CDs into the semiconductor nanoparticles (SNPs) than in their pure materials. This increase in the atomic ratio of O_v by doping with the carbon dots acts as an active center in the nanocomposite and promotes the adsorption of the GHG. Moreover, it can also narrow the band gap of the SNPs and hence improve their light absorption.[63]

3.3 Physico-chemical, mechanical, and textural characteristics of cement-based nanocomposites

Control cubic and cylindrical samples with cement (OPC) paste containing 0.08% pure CDs have been prepared according to the method described in Fig. 2. The phase composition of the cement-based nanocomposite samples was analysed *via* XRD analysis, and the results are given in Fig. 5.

For Control OPC, characteristic peaks of cement main hydration products, calcium silicate hydrate (CSH) [$2\theta = 29.56^{\circ}$, PDF #00-033-0306] and Portlandite (CH) [$2\theta = 18.17$, 34.1, and 47.2, PDF #01-087-0674] phases can be seen.

Also, characteristic peaks for unreacted anhydrous calcium silicates (C_3S and C_2S) [$2\theta = 32.29^{\circ}$] can be found.[65] For the prepared cement-based nanocomposite samples, although the characteristic main peaks of the different nanocomposites didn't appear in the XRD pattern of the OPC due to its very low percentage in the matrix, their effect was obvious on the different hydration product phases as shown in Fig. 11. Sharper characteristic peaks for CSH and CH phases can be identified in the XRD pattern of the prepared cement-based nanocomposite, while lower intensity peaks were found for the unreacted CS phase. The findings of XRD can suggest that the addition of the nanocomposites to OPC results in the acceleration of the hydration reaction while forming more crystalline hydration products.

The physico-chemical, mechanical, and textural characteristics of new manufactured cement materials have been investigated, and the results are given in Fig. 12. For mechanical properties, compressive strength values (Fig. 12a) were measured using Controls®, Itlay-compressive strength testing machine with maximum load 300 kN. The addition of 0.08% CD showed a regression in compressive strength values at early stages of hydration, *i.e.*, 3 and 7 days. But after 28 days of curing, compressive strength values of CD-OPC composite show a slight increase over blank OPC. For composites containing 0.08% nano-oxide additions, *i.e.*, SiO_2-OPC, TiO_2-OPC, and ZnO-OPC, there is a remarkable increase in the compressive strength values compared to the blank, indicating that the addition of nano-oxides accelerated the hydration reaction, leading to the formation of larger amounts of hydration products with mechanical properties, *i.e.*, calcium silicate hydrate (CSH), leading to the increase of compressive strength values.[66]

On combining nano-oxides with CD, all the composites showed compressive strength values comparable to Blank OPC (±5%), indicating that the added CDs are not significantly interfering with the mechanism of early hydration of calcium silicate phases in OPC. While at later stages of hydration, all the ratios from CDs semiconductor nanocomposites (CD-NCs) added lead to an increase in the compressive strength values by 3% for some mixes like CD and 1% CDs/SiO_2-OPC samples, and up to 20% increase in compressive strength values in 0.05% CD/TiO_2-OPC and 1% CD/ZnO-OPC. Bulk density values represented in Fig. 12b indicate that a denser structure was formed by the addition of 0.05% CD/TiO_2-OPC, 1% CD/ZnO-OPC, and 0.05% CDs/SiO_2-OPC. Together with compressive strength values, these results indicate that these additions modify and enhance the hydration reaction, forming denser hydration products that fill the pore structure and increase compressive strength values.[60]

Water absorption values (WA) represented in Fig. 12c is also an important test since they is correlated to the structural pore system. The composites with more dense structures showed lower water absorption values, while the other composites showed comparable WA% to the blank and modified OPC samples. The 0.01% CD/ZnO-OPC and 1% CD/ZnO-OPC composites also showed the highest WA%, confirming the T.P. results.[67] Moreover, the total porosity values (T.P.) represented in Fig. 12d showed that all 0.05% NCs-OPC samples have lower porosity than the blank, which is well matched with the results of bulk density and compressive strength, and implies the formation of more hydration products that filled the pore

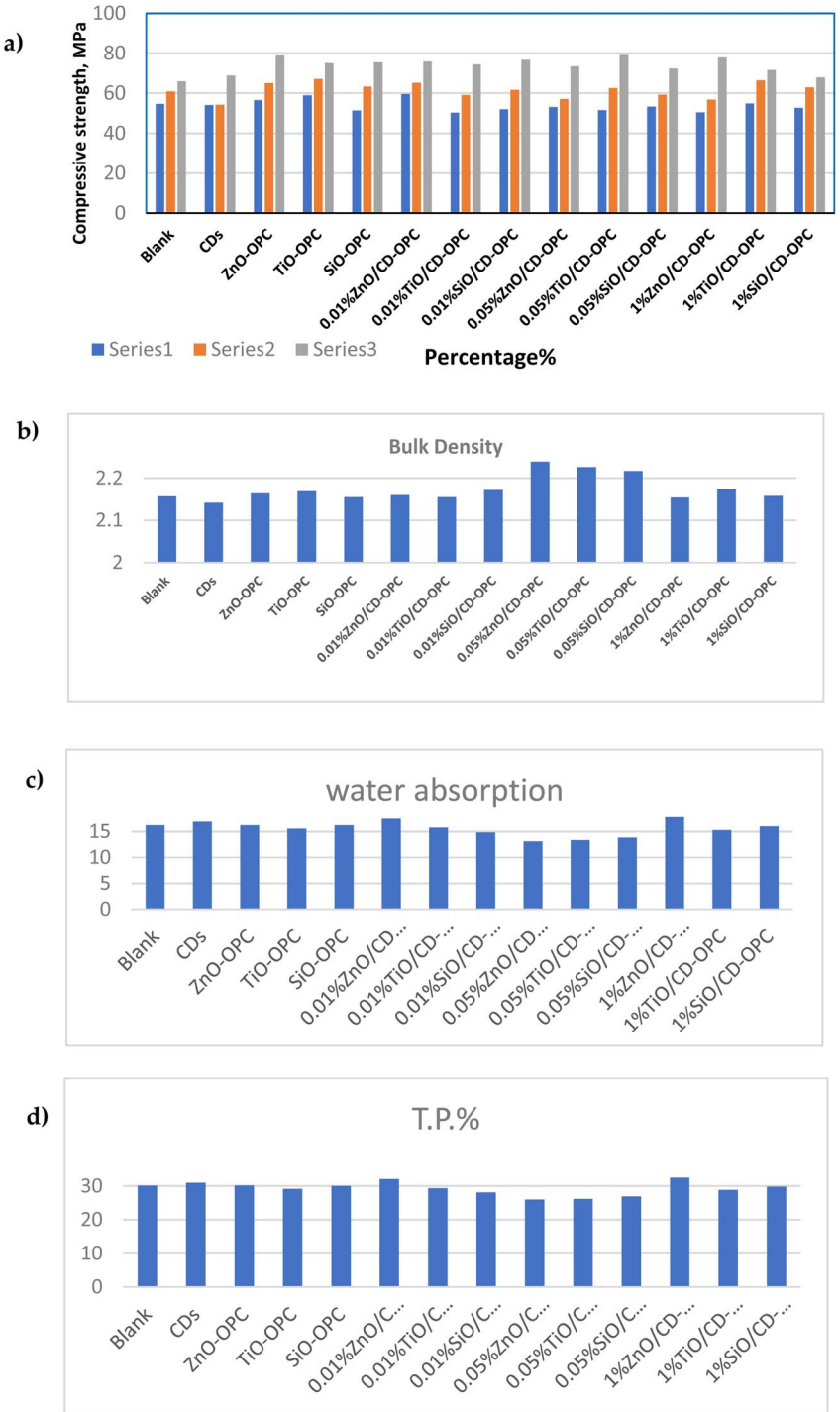

Fig. 12 Physico-chemical characteristics of the new cement building materials modified with different CD-NCs, including (a) compressive strength; (b) bulk density; (c) water absorption; and (d) total porosity.

structure. Surprisingly, although 0.01% CD/ZnO-OPC and 1% CD/ZnO-OPC have higher compressive strength values than blank, their T.P.% values indicate an increase in porosity. This can indicate that the OPC samples modified with CD-NCs enhanced the formation of more ordered semi-crystalline, other than amorphous or ill-ordered hydration products that can maintain the mechanical properties of the OPC materials.[68,69]

3.4 Photocatalytic CO_2 reduction and capturing

The photoactivity of the cement-based nanocomposite building materials to remove CO_2 gas was evaluated. Fig. 13 shows the variation of CO_2 concentration measured during a standard test (5000 ppm CO_2 inlet initial concentration; 100 mW cm^{-2} for 1 h simulated sunlight illumination; Fig. 3). The samples were kept inside the photoreactor in the dark for a period of 10 min until

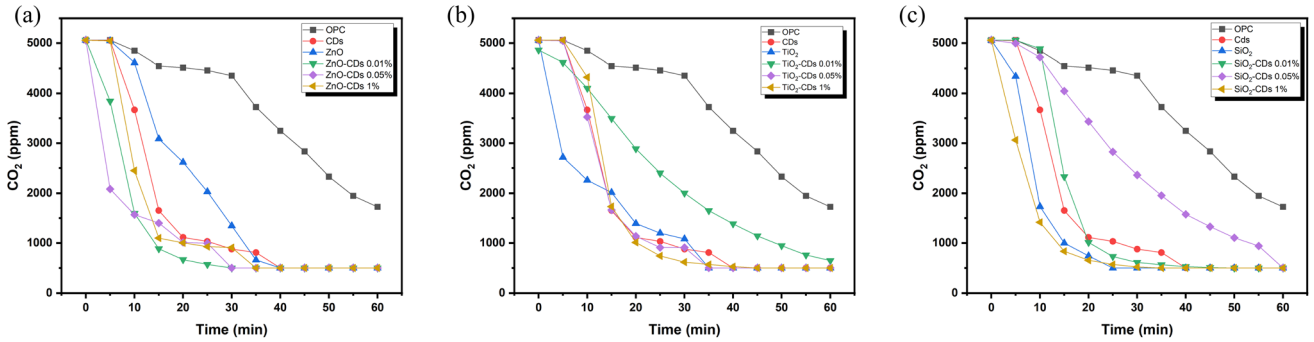

Fig. 13 CO_2 (ppm g^{-1}) reduction using cement modified with the different CDs nanocomposites under simulated sunlight illumination (a) effect of loading CDs-ZnO, (b) effect of loading CDs-TiO_2, and (c) effect of loading CDs-SiO_2 nanocomposites.

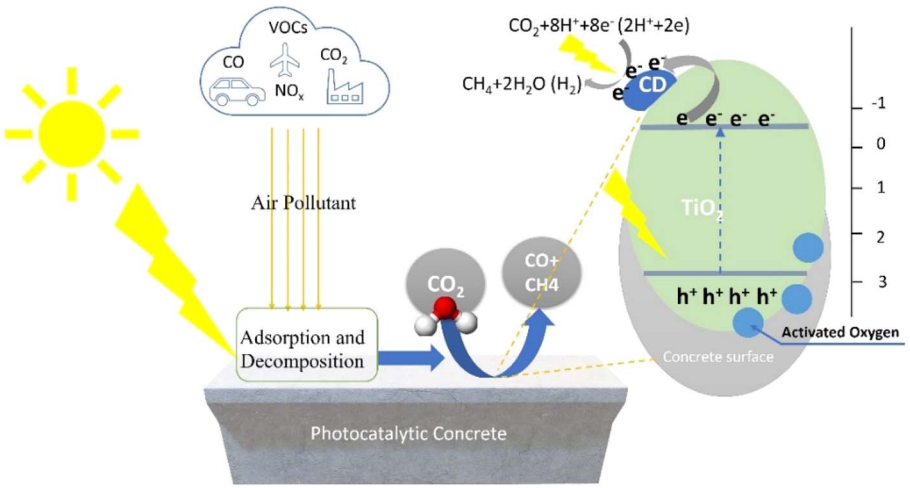

Fig. 14 A proposed mechanism for the CO_2 reduction over OPC building materials modified with CDs/SNPs under simulated sunlight illumination.

a constant concentration of the gas inlet reached 5000 ppm. Subsequently, once the samples are irradiated for approximately 60 minutes, a fast decay in the CO_2 concentration is measured in ppm g^{-1} is observed. The decay in the concentration per unit gm weight of the OPC sample was then recorded as a function of time (Fig. 13).

The results reveal that the presence of CDs nanocomposites enhances the photochemical reduction activity of the modified OPC building material. It can naturally absorb CO_2 from the surrounding atmosphere under sunlight illumination within one hour of illumination. In particular, the OPC samples modified with 0.05% CDs nanocomposites were most effective, suggesting that optimal CD-NCs concentration can boost photocatalytic activity towards GHGs reduction. This improved performance is attributed to synergistic effects between the components, enhanced light absorption and photoactivity by CD-NCs, and improved charge separation facilitated by CDs. This can be due to the enhancement of the surface area by the incorporation of the nanocomposites in the cement material. Moreover, increasing the oxygen vacancies due to the addition of a low concentration of CDs in the nanocomposites leads to enhancing their absorptivity.[64]

A proposed mechanism for the photocatalytic CO_2 reduction process over the cement modified by CDs nanocomposites can be considered and presented in Fig. 14. Firstly, when CDs-NCs are exposed to UV-vis light with higher energy than the SNPs bandgap, the electrons are excited from the valence to the CDs conduction band and create a hole (+h) at its valence band. These photogenerated positive holes react with the atmospheric water molecules to produce $OH^{\bullet}$. Subsequently, the generated electrons at the conduction band react with the oxygen of CDs and produce $O_2^{\bullet -}$, which produces a strong reducing agent for CO_2 reduction. Moreover, this charge would prevent electron–hole pair recombination and increase photocatalytic activity.[69] These reactions lead to the oxidation and decomposition of the pollutants into less harmful or harmless substances like carbon dioxide (CO_2).

3.5 Reusability

The reusability and durability of cement-based nanocomposites have been investigated over three repeated cycles, and the results are depicted in Fig. 15 and presented in Fig. 16. After 30 min, 0.05% CD-SiO_2 OPC samples exhibit CO_2 removal efficiency 90% in the first cycle, 81% in the 2nd and 60% in the 3rd

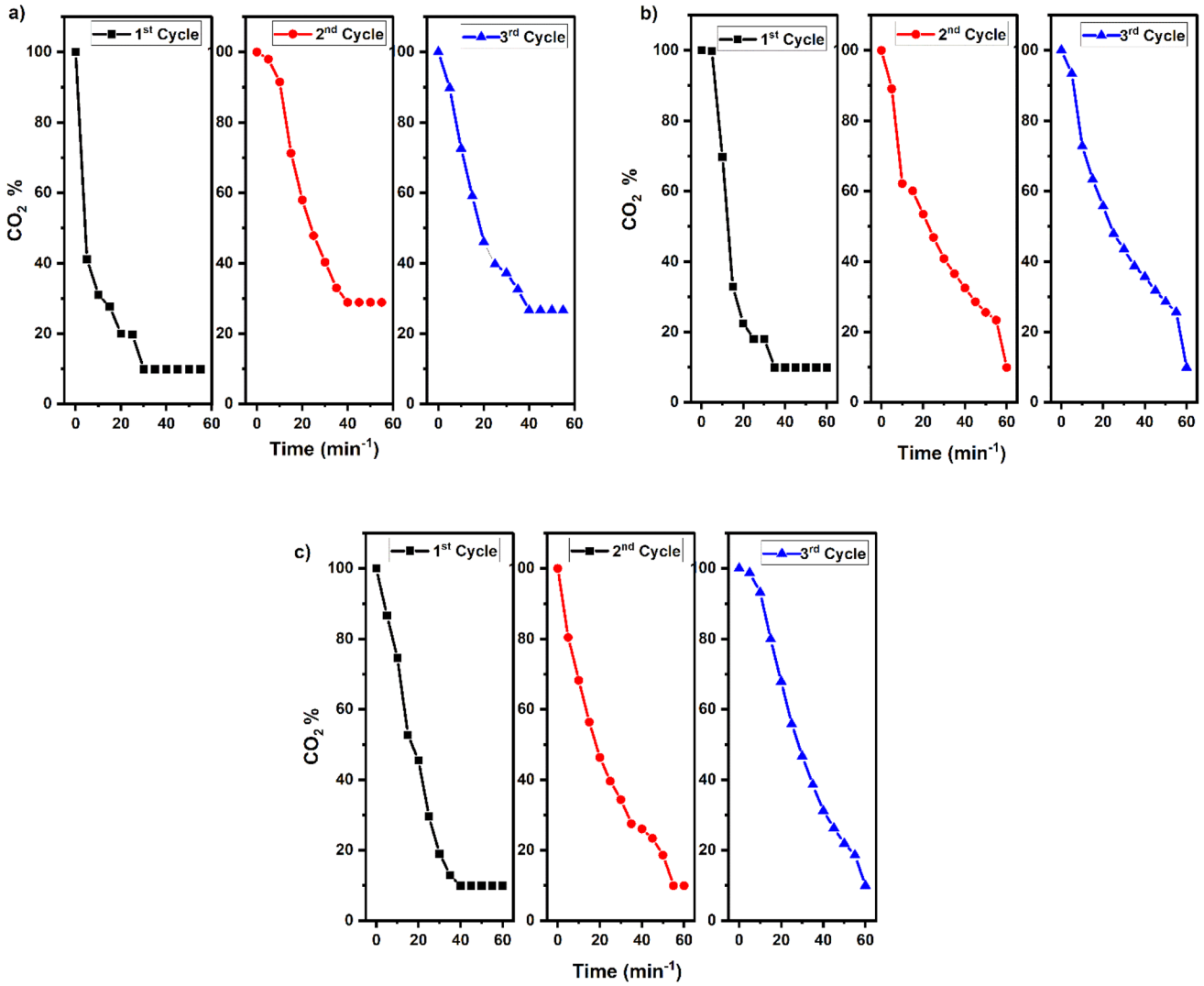

Fig. 15 CO_2 removal efficiency using (a) 0.05% CD-TiO_2, (b) 0.05% CD-ZnO, and (c) 0.05% CD-SiO_2 loaded OPC samples for 3 repeated reusability cycles under simulated sunlight illumination.

cycle (Fig. 15c). While, for the OPC samples based on 0.05% CDs-ZnO and 0.05% CDs-TiO_2, the removal efficiency were 59, 62% and 81, 56% at the 2nd and 3rd cycles, respectively (Fig. 15a and b).

These results demonstrated that the modified smart building materials that based on CD-nanocomposites exhibited a good performance for removal of green-house gases such as CO_2 with perfect activity and reusability for three repeated cycles with removal efficiency of approximately 80–90% in the 1st cycle, 60–80% in the 2nd cycle and 56–65% in the 3rd cycle (Fig. 16).

The most relevant conclusions are that these green building materials have been demonstrated as promising smart materials for carbon dioxide (CO_2) capture and conversion needed for a sustainable environment.

3.6 Toxicity assay

From the practical point of view, the cytotoxicity assay of the as-synthesized CDs was evaluated on normal human skin fibroblast cells. Human primary normal skin fibroblast cells: the hFB cell line was obtained from the Brazilian cell bank (BCRJ, Rio de Janeiro, Brazil). The cells were cultured in Dulbecco's Modified Eagle Medium (DMEM). The medium was supplemented with 10% fetal bovine serum (FBS), 2 mM L-glutamine, containing 100 units per ml penicillin G sodium, 100 units per ml streptomycin sulphate, and 250 ng per mL amphotericin B. All from Biowest, Nuaillé, France. Cells were maintained at subconfluency at 37 °C in humidified air containing 5% CO_2. All cell culture materials were obtained from SPL Life Sciences (Seoul, South Korea). All chemicals were from Sigma-Aldrich, USA, except as mentioned. The analysis was conducted at the Creative Egyptian Biotechnology Laboratory (CEB, Cairo, Egypt). Fig. 17 shows the results of the cytotoxicity analysis of CDs on the cell viability effect on normal skin fibroblast human cells for 48 h. The cytotoxicity test was measured against hFB cells for 48 h. Using the MTT (3-[4,5-dimethylthiazole-2-yl]-2,5-diphenyltetrazolium bromide) Cell Viability Assay. The cell viability% for 48 h is given in Fig. 15. It

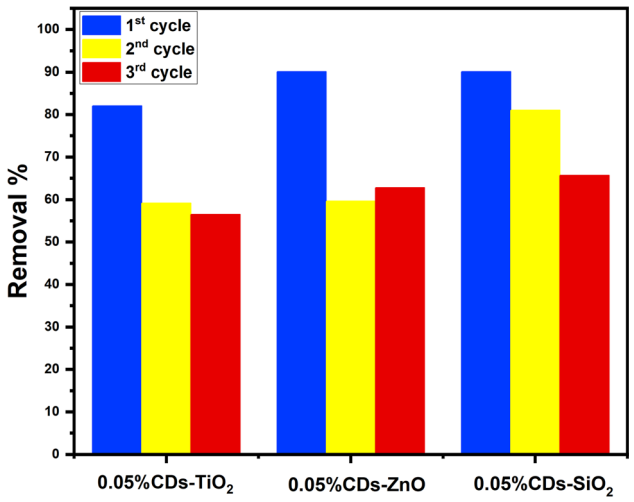

Fig. 16 Bar representation of the CO_2 removal efficiency using 0.05% CD-TiO_2, 0.05% CD-ZnO, and 0.05% CD-SiO_2 loaded OPC samples for 3 repeated reusability cycles for 30 min under simulated sunlight.

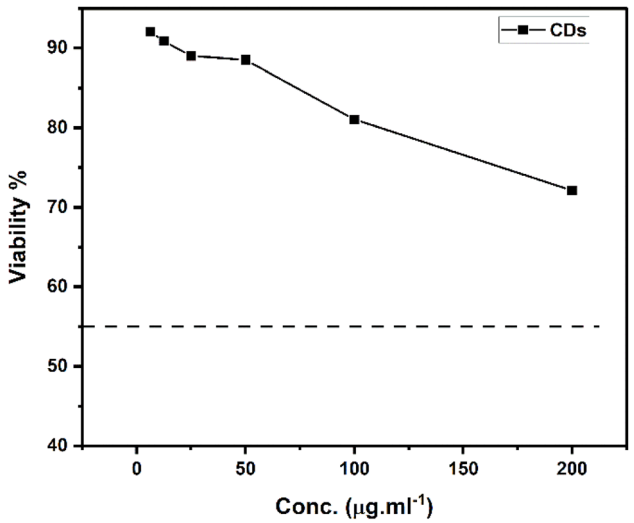

Fig. 17 Cytotoxicity of CDs on the cell viability of normal skin fibroblast human cells for 48 h.

shows a low cytotoxicity above 200 μg mL^{-1}, indicating that it's safe for use in building materials at low concentrations.

4 Conclusion(s)

The study is aimed at designing and forming nanocomposites with the basis of CDs for several multifunctional uses. Accordingly, it deals with microwave hydrothermal synthesis techniques that generate CDs nanoparticles exhibiting strong photoluminescence and good water solubility. Doping the resultant CDs with different kinds of semiconductor nanoparticles (SNPs) such as TiO_2, ZnO, and SiO_2 gave further development toward carbon dot nanocomposites (CD-NCs) with superior textural characteristics regarding surface area, porosity, as well as superior optical characteristics. The modified cement materials with these nanocomposites exhibited excellent photocatalytic performance for CO_2 reduction under sunlight simulators. The highest active cement materials modified with 0.05% CD-NCs had promising reusability for three repeated cycles. This significantly demonstrates the great potential applications of CD-NCs in cement building materials in CO_2 capturing and hence the global warming reduction.

Author contributions

The authors confirm contribution to the paper as follows: study conception and design: H. H., O. M., and M. H.; data collection: B. A., H. E., O. M., and M. H.; analysis and interpretation of results and draft manuscript preparation: H. H., O. M., B. A., and M. H. All authors reviewed the results and approved the final version of the manuscript.

Conflicts of interest

The authors declare no conflicts of interest.

Data availability

All the data investigated in this research are accessible to the corresponding author.

Supplementary information (SI) is available. See DOI: https://doi.org/10.1039/d6ra01080f.

Acknowledgements

This work is funded by the Science and Technology Development Fund (STDF), Egypt, grant no PGSG-48603 and project no. CB-42957.

References

1 L. Jasmani, R. Rusli, T. Khadiran, R. Jalil and S. Adnan, Application of nanotechnology in wood-based products industry: A review, *Nanoscale Res. Lett.*, 2020, **15**, 207, DOI: 10.1186/s11671-020-03438-2.
2 S. Khan, S. Mansoor, Z. Rafi, B. Kumari, A. Shoaib, M. Saeed, S. Alshehri and M. M. Ghoneim, A review on nanotechnology: Properties, applications, and mechanistic insights of cellular uptake mechanisms, *J. Mol. Liq.*, 2022, **348**, 118008, DOI: 10.1016/j.molliq.2021.118008.
3 I. M. Toussaint-Samat, A comparative study of research and development related to nanotechnology in Egypt, Nigeria and South Africa, *Technol. Soc.*, 2022, **68**, 101888, DOI: 10.1016/j.techsoc.2022.101888.
4 M. Du, H. Jing, Y. Gao, H. Su and H. Fang, Carbon nanomaterials enhanced cement-based composites: Advances and challenges, *Nanotechnol. Rev.*, 2020, **9**, 115–135, DOI: 10.1515/ntrev-2020-0011.
5 H. A. Gamal, M. S. El-Feky, Y. R. Alharbi, A. A. Abadel and M. Kohail, Enhancement of the concrete durability with

hybrid nano materials, *Sustainability*, 2021, **13**, 1373, DOI: 10.3390/su13031373.
6 A. Mohajerani, L. Burnett, J. V. Smith, H. Kurmus, J. Milas, A. Arulrajah and S. Horpibulsuk, Nanoparticles in construction materials and other applications, and implications of nanoparticle use, *Materials*, 2019, **12**, 3052, DOI: 10.3390/ma12193052.
7 D. Papadaki and G. Kiriakidis, Applications of nanotechnology in construction industry, in *Trends in Functional Nanoparticles*, Elsevier, 2018, DOI: 10.1016/B978-0-323-51255-8.00011-2.
8 M. Rafique, M. B. Tahir, M. S. Rafique, N. Safdar and R. Tahir, Nanostructure materials and their classification by dimensionality, in *Nanotechnology and Photocatalysis for Environmental Applications*, 2020, pp. 27–44, DOI: 10.1016/B978-0-12-821192-2.00002-4.
9 D. Roy, A. K. Srivastava, K. Mukhopadhyay and E. P. Namburi, 0D, 1D, 2D & 3D nano materials: synthesis and applications, in *Novel Defence Functional and Engineering Materials (NDFEM)*, 2024, pp. 73–91, DOI: 10.1007/978-981-99-9791-6_3.
10 Y. Zhou, J. Wang, C. Liang and F. Zheng, *Nanotechnology and Materials Science: Innovations for Industry and Infrastructure*, 2024, pp. 375–394, DOI: 10.1007/978-981-97-6184-5_11.
11 H. A. Colorado, J. C. Nino and O. Restrepo, Applications and opportunities of nanomaterials in construction and infrastructure, *Miner. Met. Mater. Ser.*, 2018, 437–452, DOI: 10.1007/978-3-319-72484-3_46.
12 S. K. Wei and G. F. Huseien, *Nanomaterials for Concrete Coating Applications*, 2022, pp. 371–386, DOI: 10.1007/978-3-031-11996-5_13.
13 K. Khan, W. Ahmad, M. N. Amin and S. Nazar, Nano-silica-modified concrete: A bibliographic analysis and comprehensive review of material properties, *Nanomaterials*, 2022, **12**, 1989, DOI: 10.3390/nano12121989.
14 R. Roychand, S. De Silva, D. Law and S. Setunge, High volume fly ash cement composite modified with nano silica, hydrated lime and set accelerator, *Mater. Struct.*, 2016, **49**, 1997–2008, DOI: 10.1617/s11527-015-0629-z.
15 N. Kumar, S. Soren, A. Nirala, N. Almakayeel, T. M. Yunus Khan and M. A. Khan, Distribution of carbon nanotubes in an aluminum matrix by a solution-mixing process, *ACS Omega*, 2023, **8**, 33845–33856, DOI: 10.1021/acsomega.3c04531.
16 S. Zhang, G. Chen, T. Qu, *et al.*, A novel aluminum–carbon nanotubes nanocomposite with doubled strength and preserved electrical conductivity, *Nano Res.*, 2021, **14**, 2776–2782, DOI: 10.1007/s12274-021-3284-4.
17 M. E. Khan, State-of-the-art developments in carbon-based metal nanocomposites as a catalyst: photocatalysis, *Nanoscale Adv.*, 2021, **3**, 1887–1900, DOI: 10.1039/D1NA00041A.
18 O. S. Ayanda, A. O. Mmuoegbulam, O. Okezie, *et al.*, Recent progress in carbon-based nanomaterials: Critical review, *J. Nanopart. Res.*, 2024, **26**, 106, DOI: 10.1007/s11051-024-06006-2.
19 A. Kuda and M. Yadav, Opportunities and challenges of using nanomaterials and nanotechnology in architecture: An overview, *Mater. Today Proc.*, 2022, **65**, 2102–2111, DOI: 10.1016/j.matpr.2022.04.653.
20 E. Llobet, Gas sensors using carbon nanomaterials: A review, *Sens. Actuators, B*, 2013, **179**, 32–45, DOI: 10.1016/j.snb.2012.11.093.
21 G. G. Abdo, M. M. Zagho, A. E. Al Moustafa, A. Khalil and A. A. Elzatahry, A comprehensive review summarizing the recent biomedical applications of functionalized carbon nanofibers, *J. Biomed. Mater. Res., Part B*, 2021, **109**, 1893–1908, DOI: 10.1002/jbm.b.34828.
22 K. Sheoran, H. Kaur, S. S. Siwal, A. K. Saini, D. V. N. Vo and V. K. Thakur, Recent advances of carbon-based nanomaterials (CBNMs) for wastewater treatment: Synthesis and application, *Chemosphere*, 2022, **299**, 134364, DOI: 10.1016/j.chemosphere.2022.134823.
23 M. F. L. De Volder, S. H. Tawfick, R. H. Baughman and A. J. Hart, Carbon nanotubes: Present and future commercial applications, *Science*, 2013, **339**, 535–539, DOI: 10.1126/science.1222453.
24 A. Rode, S. Sharma and D. K. Mishra, Carbon nanotubes: Classification, method of preparation and pharmaceutical application, *Curr. Drug Delivery*, 2018, **15**, 620–629.
25 A. K. Geim and K. S. Novoselov, The rise of graphene, *Nat. Mater.*, 2007, **6**, 183–191, DOI: 10.1038/nmat1849.
26 Y. Zhu, S. Murali, W. Cai, *et al.*, Graphene and graphene oxide: Synthesis, properties, and applications, *Adv. Mater.*, 2010, **22**, 3906–3924, DOI: 10.1002/adma.201001068.
27 O. C. Compton and S. T. Nguyen, Graphene oxide, highly reduced graphene oxide, and graphene: Versatile building blocks for carbon-based materials, *Small*, 2010, **6**, 711–723, DOI: 10.1002/smll.200901934.
28 M. M. Shokrieh, M. Esmkhani, H. R. Shahverdi and F. Vahedi, Effect of graphene nanosheets (GNS) and graphite nanoplatelets (GNP) on the mechanical properties of epoxy nanocomposites, *Sci. Adv. Mater.*, 2013, **5**, 260–266.
29 A. Gholampour, M. Valizadeh Kiamahalleh, D. N. H. Tran, T. Ozbakkaloglu and D. Losic, From graphene oxide to reduced graphene oxide: Impact on the physicochemical and mechanical properties of graphene–cement composites, *ACS Appl. Mater. Interfaces*, 2017, **9**, 43275–43286, DOI: 10.1021/acsami.7b16736.
30 O. Skorobogatova and I. Kuzmina-Merlino, Investigating the rheological and thermal response of binder modified with multi-layered reduced graphene oxide (RGO), *Constr. Build. Mater.*, 2026, **510**, 14529.
31 T. S. Qureshi and D. K. Panesar, Impact of graphene oxide and highly reduced graphene oxide on cement-based composites, *Constr. Build. Mater.*, 2019, **206**, 71–83.
32 I. Khan, K. Saeed and I. Khan, Comprehensive review of carbon-based nanostructures: Properties, synthesis, characterization, and cross-disciplinary applications, *J. Ind. Eng. Chem.*, 2025, **146**, 176–212.
33 M. A. Gatou, I. A. Vagena, N. Pippa, M. Gazouli, E. A. Pavlatou and N. Lagopati, The use of crystalline carbon-based

nanomaterials (CBNs) in various biomedical applications, *Crystals*, 2023, **13**, 1236, DOI: 10.3390/cryst13081236.

34 N. N. Joshi, J. Narayan and R. Narayan, Multifunctional carbon-based nanostructures (CBNs) for advanced biomedical applications – A perspective and review, *Mater. Adv.*, 2024, **5**, 9160–9174, DOI: 10.1039/D3MA00636K.

35 B. Marinho, M. Ghislandi, E. Tkalya, C. E. Koning and G. de With, Electrical conductivity of compacts of graphene, multi-wall carbon nanotubes, carbon black, and graphite powder, *Powder Technol.*, 2012, **221**, 351–358.

36 P. R. Bandaru, H. Yamada, R. Narayanan and M. Hoefer, The role of defects and dimensionality in influencing the charge, capacitance, and energy storage of graphene and 2D materials, *Nanotechnol. Rev.*, 2017, **6**, 421–433.

37 S. Wan, H. Bi and L. Sun, Graphene and carbon-based nanomaterials as highly efficient adsorbents for oils and organic solvents, *Nanotechnol. Rev.*, 2016, **5**, 3–22.

38 S. C. Vanithakumari, G. Sahana, A. R. Shankar and S. Ningshen, Self-cleaning graphene oxide-based superhydrophobic coating on steel for improving corrosion and biofouling resistance, *J. Sol-Gel Sci. Technol.*, 2025, **115**, 1465–1478.

39 J. P. Filipovic, M. Milenkovic, D. Kleut, K. Haddadi, M. Yasir, W. Saeed and D. B. Bogdanovic, Sustainable gamma irradiation strategy for GO and rGO modification: Impact on electromagnetic interference shielding efficiency, *Chem. Eng. J. Adv.*, 2025, **24**, 100873, DOI: 10.1016/j.ceja.2025.100873.

40 A. C. Power, B. Gorey, S. Chandra and J. Chapman, Carbon nanomaterials and their application to electrochemical sensors: A review, *Nanotechnol. Rev.*, 2018, **7**, 19–41.

41 E. Shamsaei, F. B. de Souza, X. Yao, E. Benhelal, A. Akbari and W. Duan, Graphene-based nanosheets for stronger and more durable concrete: A review, *Constr. Build. Mater.*, 2018, **183**, 642–660.

42 L. Restuccia and G. A. Ferro, Promising low cost carbon-based materials to improve strength and toughness in cement composites, *Constr. Build. Mater.*, 2016, **126**, 1034–1043.

43 M. S. Felix, R. U. H. Zamora, M. A. A. Rubio, C. C. Gallardo and J. M. H. Ramirez, Sustainable low-carbon cement: Performance enhancement with calcined natural pozzolans through compressive strength, porosity, and microstructural analysis, *Materials*, 2025, **18**, 1776.

44 H. Du, S. T. Quek and S. D. Pang, Smart multifunctional cement mortar containing graphite nanoplatelet, in *Sensors and Smart Structures Technologies for Civil, Mechanical, and Aerospace Systems*, 2013, vol. 8692, p. 869238.

45 B. Han, S. Sun, S. Ding, L. Zhang, X. Yu and J. Ou, Review of nanocarbon-engineered multifunctional cementitious composites, *Compos., Part A*, 2015, **70**, 69–81.

46 Y. Xu, J. Zeng, W. Chen, R. Jin, B. Li and Z. Pan, A holistic review of cement composites reinforced with graphene oxide, *Constr. Build. Mater.*, 2018, **171**, 291–302.

47 S. S. Volaity, B. K. Aylas-Paredes, T. Han, *et al.*, Towards decarbonization of cement industry: A critical review of electrification technologies for sustainable cement production, *npj Mater. Sustain.*, 2025, **3**, 23.

48 L. Prasittisopin, R. Nganglumpoon, C. Thongchom and J. Panpranot, Systematic review and thematic analysis of the utilization of carbon quantum dots (CQDs) in construction materials, *J. Mater. Sci. Eng.*, 2025, **20**, 1.

49 S. Agarwal and S. Bhatia, Carbon dots: Emerging green nanoprobes and their diverse applications, in *Functionalized Nanomaterials for Catalytic Application*, 2021, pp. 417–492.

50 J. Zhang, Q. Fu, S. Sun, K. Zhang and M. Yue, Carbon dots composite luminescent materials: Design, optical properties, and applications, *Nano Mater. Sci.*, 2025, S2589965125000625, DOI: 10.1016/j.nanoms.2025.06.002.

51 H. Qu, S. Qian, X. Liu, R. Gao, Z. Wang, C. Zheng and Z. Zhang, Carbon dots as a superior building nanomaterial for enhancing the mechanical properties of cement-based composites, *J. Build. Eng.*, 2022, **52**, 104523, DOI: 10.1016/j.jobe.2022.104523.

52 F. Josephraj, A. K. N., V. V. Nandini, S. S. B. and V. Karthik, Performance evaluation of carbon quantum dots impregnated glass ionomer cement to avoid peri-implant disease, *Biomed. Mater.*, 2024, **19**(3), 035040, DOI: 10.1088/1748-605X/ad407b.

53 T. M. Sheikh, M. P. Anwar, K. Muthoosamy, J. Jaganathan, A. Chan and A. A. Mohamed, The mechanics of carbon-based nanomaterials as cement reinforcement—A critical review, *Constr. Build. Mater.*, 2021, **303A**, 124441, DOI: 10.1016/j.conbuildmat.2021.124441.

54 W. J. Long, A. N. Zhong, S. Y. Zheng and C. He, Effects of a novel carbon nanomaterial on hydration, mechanics, and chloride binding of cement composites, *Carbon*, 2024, **221**, 118933, DOI: 10.1016/j.carbon.2024.118933.

55 O. A. Mbrouk, M. Fawzy, H. M. El-Shafey, M. Saif, H. Hafez and M. S. A. A. Abdel Mottaleb, Green synthesized plasmonic Pd–ZnO nanomaterials for visible light-induced photobiogas production from industrial wastewater, *Appl. Organomet. Chem.*, 2022, 36, DOI: 10.1002/aoc.6807.

56 O. Mbrouk, M. Fawzy, H. M. El-Shafey, M. Saif, M. S. A. A. Mottaleb and H. Hafez, Viable production of hydrogen and methane from polluted water using eco-friendly plasmonic Pd–TiO_2 nanocomposites, *RSC Adv.*, 2023, **13**(2), 770–780, DOI: 10.1039/D2RA07442G.

57 M. M. Abomughaid, Bio-fabrication of bio-inspired silica nanomaterials from orange peels in combating oxidative stress, *Nanomaterials*, 2022, **12**, 3236.

58 British Standards Institution, *BS EN 196-1:2016 Methods of Testing Cement – Determination of Strength*, BSI, London, 2016.

59 Z. L. Wu, P. Zhang, M. X. Gao, C. F. Liu, W. Wang, F. Leng and C. Z. Huang, One-pot hydrothermal synthesis of highly luminescent nitrogen-doped amphoteric carbon dots for bioimaging from Bombyx mori silk–natural proteins, *J. Mater. Chem. B*, 2013, **1**, 2868–2873, DOI: 10.1039/C3TB20418A.

60 S. Yadav, A. Kumar and D. Kumar, Photodegradation of methylene blue onto boron/phosphorous modified carbon

dots prepared by hydrothermal and microwave-assisted methods, *Mater. Sci. Energy Technol.*, 2023, **6**, 260–266.

61 C. R. Thara, B. K. Korah, S. Mathew, B. K. John and B. Mathew, Dual mode detection and sunlight-driven photocatalytic degradation of tetracycline with tailor-made N-doped carbon dots, *Environ. Res.*, 2023, **216**, 114450, DOI: 10.1016/j.envres.2022.114450.

62 M. D. Malitha, M. T. H. Molla, M. A. Bashar, D. Chandra and M. S. Ahsan, Fabrication of a reusable carbon quantum dots (CQDs) modified nanocomposite with enhanced visible light photocatalytic activity, *Sci. Rep.*, 2024, **14**, 17976.

63 J. J. Xu, Y. N. Lu, F. F. Tao, P. F. Liang and P. A. Zhang, ZnO nanoparticles modified by carbon quantum dots for the photocatalytic removal of synthetic pigment pollutants, *ACS Omega*, 2023, **8**, 7845–7857, DOI: 10.1021/acsomega.2c07591.

64 A. Wang, X. Xiao, C. Zhou, F. Lyu, L. Fu, C. Wang and S. Ruan, Large-scale synthesis of carbon dots/TiO_2 nanocomposites for the photocatalytic color switching system, *Nanoscale Adv.*, 2019, **1**, 1819–1825.

65 M. Ramadan, S. M. A. El-Gamal, M. M. Wetwet and M. M. Hazem, Amelioration of antimicrobial, radiation shielding, and thermal stability of Portland cement composites using hematite nanoparticles, *Constr. Build. Mater.*, 2024, 421.

66 M. A. Mousavi, A. Sadeghi-Nik, A. Bahari, C. Jin, R. Ahmed, T. Ozbakkaloglu and J. de Brito, Strength optimization of cementitious composites reinforced by carbon nanotubes and titania nanoparticles, *Constr. Build. Mater.*, 2021, **303**, 124510, DOI: 10.1016/j.conbuildmat.2021.124510.

67 M. Singh, B. Saini and H. D. Chalak, Performance and composition analysis of engineered cementitious composite (ECC): A review, *J. Build. Eng.*, 2019, **26**, 100851, DOI: 10.1016/j.jobe.2019.100851.

68 M. Ramadan, M. Kohail, A. A. Abadel, Y. R. Alharbi, A. M. Soliman and A. Mohsen, Exploration of mechanical performance, porous structure, and self-cleaning behavior for hydrothermally cured sustainable cementitious composites, *J. Mater. Res. Technol.*, 2023, **25**, 3998–4019, DOI: 10.1016/j.jmrt.2023.06.224.

69 R. Gusain, N. Kumar and S. S. Ray, Metal oxide-based nanocomposites for photocatalytic reduction of CO_2, in *Advanced Materials for a Sustainable Environment*, 2022, pp. 293–315, DOI: DOI: 10.1201/9781003206385-13.